Methodology of Preliminary Design and Performance of a Axial-Flow Fan through CFD

Ramirez Camacho, R. G.; Oliveira, W.; dos Santos, E. C.; da Silva, E. R.; Arispe, T.; da Costa, C. E. A.; dos Reis, T. C. A

***Abstract*—**It presents a preliminary design methodology of an axial fan based on the lift wing theory and the potential vortex hypothesis. The literature consider a study of acoustic and engineering expertise to model a fan with low noise. Axial fans with inadequate intake geometry, often suffer poor condition of the flow at the entrance, varying from velocity profiles spatially asymmetric to swirl floating with respect to time, this produce random forces acting on the blades. This produce broadband gust noise which in most cases triggers the tonal noise. The analysis of the axial flow fan will be conducted for the solution of the Navier-Stokes equations and models of turbulence in steady and transitory (RANS - URANS) 3-D, in order to find an efficient aerodynamic design, with low noise and suitable for industrial installation. Therefore, the process will require the use of computational optimization methods, aerodynamic design methodologies and numerical methods as CFD- Computational Fluid Dynamics. The objective is the development of the methodology of the construction axial fan, provide of design the geometry of the blade, and evaluate aerodynamic performance.

***Keywords*—**Axial fan design, optimization, CFD, Preliminary Design.

I. INTRODUCTION

The theory of flow in linear cascades find broad application in the aerodynamic design of rotors and stators of axial flow machines, both motor (turbine) and generators (pump). From 1940, the calculation of axial turbomachinery also started to incorporate some elements of support wing theory called (developed for aircraft flight). Although this flight theory has been developed for the study of a "blade" isolated (an airplane wing), it can be satisfactorily applied to axial machines having fewer blades, such as pumps, fans and turbines. Propping up the good results that have been obtained, it can be said that, the "lift wing theory" is a systematic tool of axial turbomachinery design. It is customary to call it, also, of the blade element theory.

In this sense, will be presented elements of lift wing theory (airfoils) and some theoretical foundations of linear cascades. The relationship between these two treatments will establish a basis for calculating of axial machines. The issue of radial balance is also addressed because of its practical relevance. Finally, exemplifies the usefulness of this material with an axial fan design and a hydraulic turbine type propeller [5].

The main objectives to achieve efficient designs fans is to reduce the noise levels associated with the rotor aerodynamics. Many companies that use fans must comply with environmental laws requiring appropriate sound levels in this respect the fans of the blades projects should be conditioned so attenuate noise levels avoiding the separation of boundary layers and the generation of flow fields with high vorticity.

The theory of free vortex, allows for axial fans projects with minimal losses, where the specific energy is evenly distributed along the blade height. This paper presents the design methodology aiming at a greater hydraulic efficiency, resulting in quieter fans.

II. METHODOLOGY

A. Theoretical foundations in linear cascades

The theory of the potential flow around aerodynamic shapes can be applied satisfactorily to determinate the pressure distribution and lift force at low angles of attack of low width and low cambered shapes. However, the drag force can't be predicted with this theory. In the practical applications of design and analysis, it is necessary to apply other methods. For example, viscous calculations like Navier-Stokes implemented in CFD programs or simpler viscous/non-viscous interaction programs. Another alternative is to use experimental data, obtained by wind tunnel experiments.

Figure 1 show is an axial rotor machine, a cylindrical cutting and development in this cascade radio station. As a first approximation, it is assumed that the flow takes place in these

Ramirez Camacho, R. G., was with Federal University of Itajubá, Campus Prof. José Rodrigues Seabra . Av. BPS, 1303, Pinheirinho, Itajubá – MG. Telephone: (35) 3629 – 1101. PO box 50 ZIP code: 37500 90; (e-mail: ramirez@unifei.edu.br).

Oliveira, W., was with was with Federal University of Itajubá, Campus Prof. José Rodrigues Seabra. Av. BPS, 1303, Pinheirinho, Itajubá – MG. Telephone: (35) 3629 – 1101. PO box 50 ZIP code: 37500 90; (e-mail: waldir@unifei.edu.br).

Dos Santos, E. C., was with Federal University of Pará. St: Augusto Corrêa, 01 - Guamá. ZIP code 66075-110. PO box 479. Belém - Pará – Brazil; (e-mail eraldocs@hotmail.com).

Da Silva, E. R., was with Federal University of Itajubá, Campus Prof. José Rodrigues Seabra. Av. BPS, 1303, Pinheirinho, Itajubá – MG. Telephone: (35) 3629 – 1101. PO box 50 ZIP code 37500 90; (e-mail: ednaunifei@yahoo.com.br).

Arispe, T., was with Federal University of Itajubá, Campus Prof. José Rodrigues Seabra . Av. BPS, 1303, Pinheirinho, Itajubá – MG. Telephone: (35) 3629 – 1101. PO box 50 ZIP code 37500 90; (e-mail: tani.arispe86@gmail.com).

da Costa, C. E. A., was with BRENTECH ENERGIA S/A, Jardim Ipanema, Aparecida de Goiânia - GO. Goiás; (e-mail: carlos@brentech.com.br).

dos Reis, T. C. A., was with BRENTECH ENERGIA S/A, Jardim Ipanema, Aparecida de Goiânia – GO. Goiás.

cylindrical surfaces without radial component can thus be studied in the corresponding linear cascade.

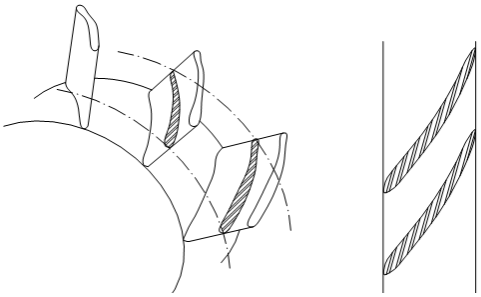

(a) (b)

Fig 1. (a) Rotor axial flow machine, cylindrical cutting, (b) and cascade representation.

The Figure 2a and b show more details of the linear cascade and velocity triangles. The cascade is composed of identical and equally spaced airfoils.

- Spacing between the profiles is called the pitch. *t*;
- Length of the chord is *l*;
- Stagger angle is define as β.

The flow approaches the cascade with uniform velocity $\boldsymbol{w}_3$. To be deflected by the blades, the flow comes out with uniform velocity $\boldsymbol{w}_6$. The vector $\boldsymbol{w}_\infty$ average speed is defined by $w_\infty = (\boldsymbol{w}_3 + \boldsymbol{w}_6)/2$; its usefulness will become apparent hereinafter. In what follows, it is assumed still dimensional flow (2D), permanent (in relation to the mobile cascade), incompressible and non-viscous (potential).

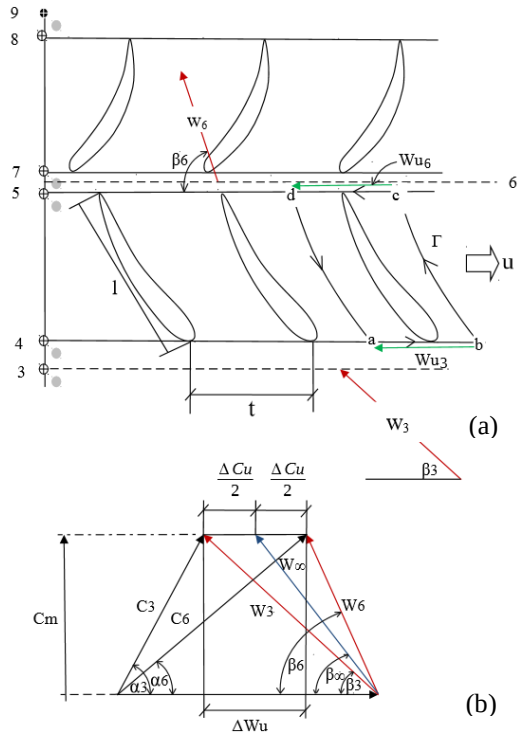

Fig. 2 (a) Linear axial cascade; (b) Velocity triangles (pump).

What flow lifting force exerted on the profile, is the most responsible for energy transfer between the fluid and the shovel, it is due to the development of Γ circulation around the profile . Due to the flow of the periodicity hypothesis for each channel formed by two consecutive blades, it is considered to calculate the circulation effect, the lines *b-c* and *d-a* are symmetrical, in such a manner to cancel the corresponding circulations. It has then:

$$\Gamma = \oint_{abcda} \vec{w} \cdot d\vec{s} = -\int_{ab} w_{u3}\, ds + \int_{cd} w_{u6}\, ds \qquad (1)$$

Resulting

$$\Gamma = -w_{u3}\, t + w_{u6}\, t = t\,\Delta w_u = t\,\Delta c_u \qquad (2)$$

Now, applying the equation of the amount of motion in the *abcda* volume, in integral form, can be determinate the axial (z) and circumferential (u) forces which the blade exerts on the fluid and vice versa, using the Reynolds Transport Theory.

$$\vec{F}_{ext} + \int_{VC} -\vec{a}^{*}\, dm = \frac{d}{dt}\int_{VC} \vec{w}\, dm + \oint_{SC} \vec{w}\, d\dot{m} \qquad (3)$$

$$\vec{F}_{pá} = \vec{F}_{pá,u} + \vec{F}_{pá,z} = b\,\rho\, w_\infty\, \Gamma\,(\cos\beta_\infty\, \hat{k} + sen\beta_\infty\, \hat{e}_\theta) \qquad (4)$$

$$F_{pá,u} = b\rho\, w_\infty \Gamma sen\beta_\infty \qquad (5)$$

Although the previous deduction has been made considering a motor cascade, the results are valid in general as long as the friction effects are neglected (ideal flow). Those results correspond to the Kutta-Joukowsky theorem which, for the linear cascades can be enounced as: "The force $F_{pá}$ due to a potential, incompressible and permanent flow over a cascade disposed airfoil is perpendicular to the vector $\boldsymbol{w}_\infty = (\boldsymbol{w}_3 + \boldsymbol{w}_6)/2$. $\boldsymbol{w}_3$ and $\boldsymbol{w}_6$ are the velocities before and after the cascade, respectively". The magnitude of this force, per unit of width, is $F_{pá}/b = \rho\, w_\infty\, \Gamma$, where ρ is the density of the fluid and Γ is the circulation around the airfoil.

That's why it was useful to define $\boldsymbol{w}_\infty = (\boldsymbol{w}_3 + \boldsymbol{w}_6)/2$, because with this definition we recover the Kutta-Joukowsky theorem applied to airfoils in cascade. To the flow around an airfoil profile turbomachine blade, the velocity related to the incident velocity in a lift wing is the mean velocity $\boldsymbol{w}_\infty = (\boldsymbol{w}_3 + \boldsymbol{w}_6)/2$. Figure 3 represents the situation for the case of a motor machine. δ is the angle of attack (angle between $\boldsymbol{w}_\infty$ and the chord direction). The mounting angle, β, is calculated as $\beta = \beta_\infty - \delta$. In generator machines, $\beta = \beta_\infty + \delta$.

The force $\boldsymbol{F}_{pá}$ is called lift force due to the wing theory (isolated airfoil). In the ideal flow, this is the only acting force, perpendicular to $\boldsymbol{w}_\infty$. In the real case, due to the viscous friction effects and boundary layer separation, a parallel component of the force appears so that $\boldsymbol{F}_{pá}$ becomes similar to the representation in Figure 4.

This parallel component is called drag force. We will use to following denotation: F_S = lift force, F_A = drag force. The proportion F_A/F_S is called slip coefficient. In an airfoil, the purpose is to obtain little values for this coefficient within the

operation conditions. This way, we'll have $F_A << F_S$, $tg\varepsilon = F_A/F_S \approx \varepsilon$, $F_{pá} \approx F_s$.

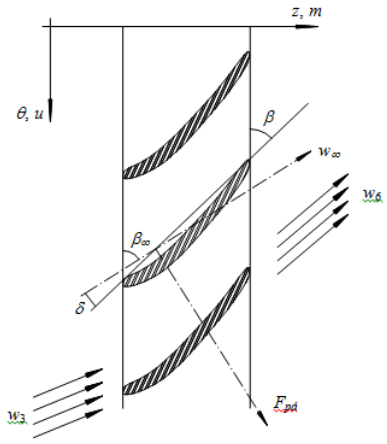

Fig. 3 Illustration of the Kutta-Joukowsky theorem applied to cascade airfoils.

This parallel component is called drag force. We will use to following denotation: F_S = lift force, F_A = drag force. The proportion F_A/F_S is called slip coefficient. In an airfoil, the purpose is to obtain little values for this coefficient within the operation conditions. This way, we'll have $F_A << F_S$, $tg\varepsilon = F_A/F_S \approx \varepsilon$, $F_{pá} \approx F_s$.

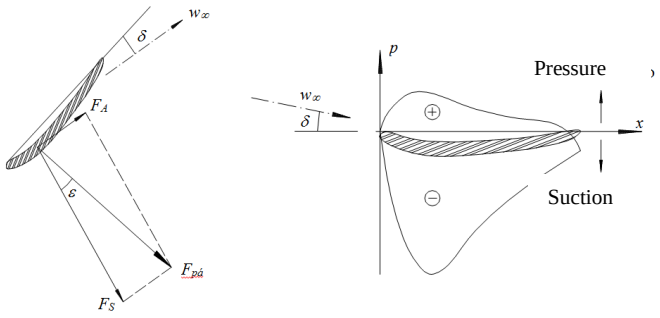

Fig. 4 Forces over an airfoil and typical pressure distribution on airfoil

The Figure 5a and b, show the typical forms of the aerodynamics characteristic by profiles, used fix values of the y_{max} / ℓ and R_e .

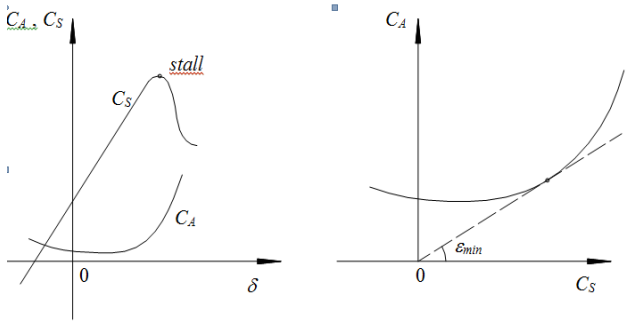

Fig. 5 Aerodynamics characteristics, (a) C_A vs. δ and C_S vs. δ; (b) Polar diagram, show the concept in ε_{min}.

The mean goals in the profile aerodynamics in operation is present low values for the drag coefficient, in this sense, is important the design in the optimal point (see Figure 7). Each profile have an optimal point in ε_{min}. This point can be obtained by diagram polar, by drawing the radius vector (from the source 0.0) tangent to the C_A x C_S (drag x lift) and measuring the angle between this radius vector and the axis C_S. All other vectors rays that intersect the curve C_A x C_S present angles ε higher.

The Figure 6 and 7 show results the aerodynamics comportment of the profile NACA 2412.

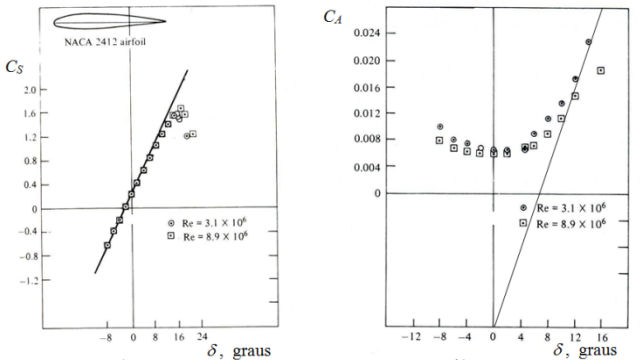

Fig. 6 Profile test results NACA 2412 [1]

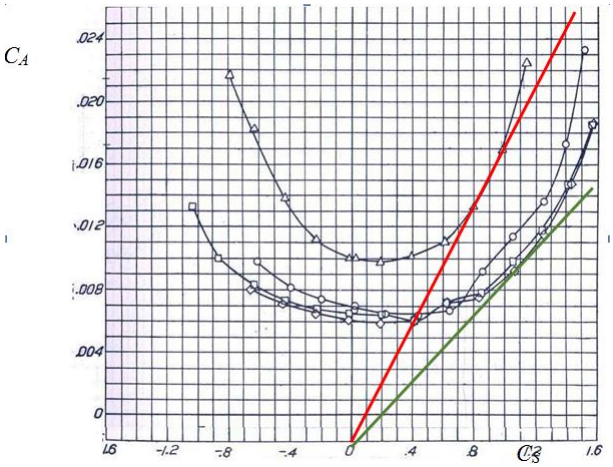

Fig. 7 Polar diagram NACA 2412 profile

For the calculation of flow machines, according to the theory of lift wing, one must know the C_S x δ functions for "profiles candidates". Analyzing the experimental results, it is seen that the influence of Reynolds number on C_s is small, a certain range of y_{max} / ℓ and δ (over C_A, however, the influence is greater). It also notes that $C_S = f(\delta)$is linear in good range of angles of attack. In general, experience shows that the following correlation profile is a typical family: [2][6].

$$C_s = C_s(y_{\max} / \ell, \delta) \approx a\frac{y_{\max}}{\ell} + b\delta \qquad (6)$$

In Equation (6) a and b are numerical constants for a particular family of profiles; y_{max} / ℓ is the maximum relative thickness. For sufficiently thin and slightly curved airfoil, the constant $b = (d\, C_S / d\delta)$ is approximately 2π, a result that can be

obtained analytically within the call theory of thin airfoil. It should be noted also that the way to Cs is the result of the superposition of the effects of the profile geometry (a y_{max} / ℓ) and the angle of attack ($b\delta$).

The profile Gottingem, NACA and Munk and your coordinates widely used in hydraulic flow machines can be found in [2][6]. And the relationships between angle of attack an lift.

Table I - Relations between angle of attack and lift Coefficient [2]

$C_s = 4.8\frac{y_{max}}{L} + 0,092\,\delta$	428,686,364,480
$C_s = 4.4\frac{y_{max}}{L} + 0,092\,\delta$	408,490,436,387
$C_s = 4.0\frac{y_{max}}{L} + 0,092\,\delta$	622,623,624,384
$C_s = 5.0\frac{y_{max}}{L} + 0,092\,\delta$	608,609,610 Circular segment
$C_s = 1.30\frac{e_{max}}{L} + 0,106\,\delta$	Munk profile
$C_s = 1.08\frac{e_{max}}{L} + 0,106\,\delta$	NACA 23012

III. RESULTING CONDITION OF THE CASCADE THEORY AND THE WING LIFT THEORY

Considering the circulation effect, Γ, in Eq.(2), the force over blade, the lift coefficient calculation, and also remembering that $F_A \approx F_S$ at the optimal operation region of the profiles, it has that:

$$F_s = b\rho\, w_\infty t\Delta c_u = bC_s \frac{1}{2}\rho w_\infty^2 \ell \qquad (7)$$

$$C_s\ \frac{\ell}{t} = \frac{2\Delta c_u}{w_\infty} \qquad (8)$$

This expression constitutes the axial turbomachinery calculation basis, referring to the wing lift theory. In this equation, relate to quantities obtained in the flow velocity triangles with the desired characteristics for the dimensionless cascades profiles. This is very important in the aerodynamic design of rotors and stators in cascade of axial flow machines [3],[4].

Briefly, is mentioned a sequence for a calculation for axial machine with aid this equation.

a) Initially are determined the diameters D_e, D_i , with the use of *Cordier* diagram curves type [2];
b) Are drawn the velocities triangles for each radial station;
c) With $Y_{pá}$ (= $u\Delta c_u$), are calculated the values $C_S\ \ell / t$;
d) Determined solidity ratio (ℓ / t), it proceed to obtain the values of C_S;
e) Calculated the thickness y_{max} (based in the material strength), are determined the attack angles δ;
f) And finally are calculated the construction of the stagger angles β.

IV. THE RADIAL EQUILIBRIUM CONDITION

The equation for the quantity of movement at the radial direction is also known as the radial equilibrium equation. In axial flow machines, this equation plays a key role in establishing the velocity distributions. In this approach, it will be taken in count, only a solution for the radial equilibrium equation, namely the potential vortex solution: case commonly adopted in design, but it deserves important observations.

The radial equilibrium equation can be obtained in the manner as follows. It is assumed a flow with axial symmetry and incompressible. Despising the viscous forces and radial velocity component, that is, assuming a purely axial flow at the meridional projection. Admitting even in the absolute flow at the stator a permanent regime and relative steady flow at the rotor.

Applying the second Newton law for the movement, to a fluid element represented at the Fig. 8 it has that:

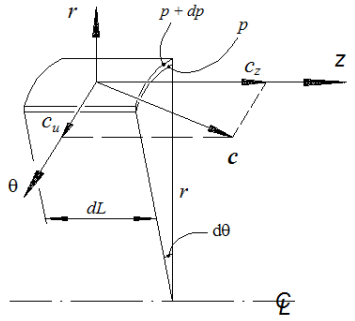

Fig. 8 Fluid element in the enclosure between the distributor and the rotor.

The radial equilibrium condition:

$$\frac{dp}{dr} = \rho\frac{c_u^2}{r} \qquad (9)$$

That is the quantity of movement equation at the direction *r*, called of the radial equilibrium equation. Using ahead the *Bernoulli* equation for the rotor:

$$\frac{p}{\rho} + \frac{w^2}{2} - \frac{u^2}{2} = \text{cte.} \qquad (10)$$

Where the gravitational effect is despised. Then applying the differentiation, it has that;

$$\frac{dp}{\rho} + \frac{dw^2}{2} = 0 \qquad (11)$$

Note that, it was previously despised the radial velocity component, it was admitted implicitly parallel current lines to the machine axis (reasonable as the first approximation in axial turbomachinery); therefore, $u = \omega r$ is assumed constant over of a given current line.

From the velocities triangles and the Euler equation, it has that:

$$Y_{pá} = u(c_{u4} - c_{u5}) = \frac{c_4^2 - c_5^2}{2} + \frac{w_5^2 - w_4^2}{2} \quad (12)$$

and,

$$dY_{pá} = -d(uc_u) = -\frac{dc^2}{2} + \frac{dw^2}{2} \quad (13)$$

Do the imposition $Y_{pá}$ = constant, and Eq.(13) (Uniform specific work through the ratio), it obtains:

$$dY_{pá} = 0\,,\ rc_u = \text{cte.}\,(\text{Potential Vortex}),\ dc^2 = dw^2 \quad (14)$$

In the other hand,

$$d(rc_u) = c_u dr + r dc_u = 0 \quad \Rightarrow \quad c_u dr = -r dc_u \quad (15)$$

Concatenating the radial equilibrium (9) and Bernoulli equation (10), then:

$$\frac{c_u}{r} c_u\, dr = -\frac{dw^2}{2} \quad (16)$$

Considering the Eqs. (15) and (14c), reducing to:

$$\frac{c_u}{r}(-r\, dc_u) = -\frac{dc^2}{2} \quad (17)$$

that is:

$$d(c^2 - c_u^2) = 0 \quad (18)$$

or yet :

$$dc_m^2 = 0 \quad \Leftrightarrow \quad c_m = \text{constant.} \quad (19)$$

Having, $Y_{pá}$ = constant $\Rightarrow$ rc_u = constant e c_m = constant. In a pure axial flow hydraulic machine. Inversely, making the assumption c_m = constant, could be proved $Y_{pá}$ = constant.

Could be conclude that in this manner c_m = constant. $\Leftrightarrow$ Y_{Pa} = constant. (rc_u = constant), in an axial hydraulic flow machine in accordance with the radial equilibrium condition. The potential vortex hypothesis is in fact widely used in turbine designs, pumps and axial fans, it is an extremely simple solution for the radial equilibrium equation with uniform distributions for the meridional velocity and specific work. However, it is only checked in practice the radial twisting vanes (distributor fins) really ensures the formation of the "potential vortex" in the enclosure between the distributor and the rotor. For this, the outlet angle α_2 should grow hub to the tip such that, together with the meridional velocity and the angular deviation of the flow at the cascades outlet in each radial station, to obtain rc_{u2} = constant. If this is not the case, where the meridional velocity distribution is not uniform along the radius as well as the distribution of the specific work of the blades. Moreover, the potential vortex condition is not necessarily the optimal setting for the flow field. Therefore, the correct radial balance should be considered in order to obtain more realistic and optimized velocities profiles.

In the case of axial fans, where can be present cube ratios (D_i / D_e) very small (less than 0.4). Other types of "vortex" should be assumed because it is impracticable to obtain the potential vortex (very strong twists near to the cube).

V. RESULTS

The axial fan chosen for design have the characteristics showed in Table II. Was considered with design parameter the characteristics of the axial fan of series 660/9-9/PAG/2ZL by MultiWing®. The Table III presents the preliminary calculation for development of the geometry of axial fan.

Table II Design Parameters for axial fan

Design Parameters		
Flow	Q (m^3/s)	9.18
Total pressure differential	Δ_{pt} (mmH_2O)	51.6
Rotation	n (rpm)	1770
Air density	ρ (kg/m^3)	1.2
Blade number	N_{pa}	9
Hydraulic efficiency	η_h (%)	80

Table III Preliminary Calculation to define the design condition

Preliminary Calculation		
Total Pressure Differential	Δ_{pt} (Pa)	506.20
Specific work	Y (J/kg)	421.83
Hydraulic power	Ph (kW)	4646.88
Rotation	n (rps)	29.50
Shaft Power	Pe (kW)	7376.00
Specifc rotation to flow	n_{qA}	960.26
Diameter Coefficient		2.02
Lightness Coefficient		1.04
D_i/D_e relation		0.3485

The table IV presents full calculation for each station of the axial fan, distributed from internal diameter to external diameter, with the triangles velocity respectively. The base profile chosen was GÖ 480.

VI. CFD ANALYSES

Flow Simulations carried out considering the data obtained with methodology of design developed. The hypothesis as, relative steady flow, incompressible and isothermal.

The automatic geometry and computational grid generation was constructed by Tcl/Tk commands, written by scripts that are interpreted through the commercial program ICEM CFD®.

The Simulation performed for this study does not consider the tip clearance, this issue will be taken into consideration in future work. Due to the fact that the flow field is repeated for each blade, it is not necessary to model the complete rotor for simulation. Therefore, the mesh is generated only in the field related to a blade, which represents 1/9 of the full domain (9 axial rotor blades)[7].

In Figures 9a and 9b can be observed the rotor geometries and complete periodic channel.

Flow Simulations carried out considering the data obtained with methodology of design developed. The hypothesis as, relative steady flow, incompressible and isothermal.

Table IV Calculations for mounting profiles distributed in 11 stations, from GÖ 480 base profile.

GÖ 480	I		II	III	IV	V	VI	VII	VIII	IX	X	XI	XII	XIII	XIV	XV	XVI	XVII	XVIII	XIX	XX
Station	D	D	u	$\Delta C_u C_{u6}$	α_6. α_7	w_∞	$\beta\infty$	$C_s l/t$	l/t	t	l	C_s	y_{max}	y_{max}/l	*Profile*	δ	β	C_o	*Re*	ε	τ
_	mm	m	m/s	m/s	°	m/s	°	_	_	mm	mm					°	°		10^5		
HUB	230	0.230	21.32	24.74	50.99	31.83	73.67	1.55	1.49	80.29	120	1.04	13.20	0.110	GÖ 480	5.57	79.24	0.94	2.7	0.019	0.420
E1	273	0.273	25.30	20.84	55.69	33.97	64.02	1.23	1.23	95.29	117	1.00	12.87	0.110	GÖ 480	5.12	69.15	0.94	2.8	0.020	0.588
E2	316	0.316	29.29	18.00	59.48	36.66	56.41	0.98	1.03	110.30	114	0.95	12.54	0.110	GÖ 480	4.59	61.00	0.94	2.9	0.021	0.693
E3	359	0.359	33.27	15.85	62.58	39.69	50.31	0.80	0.89	125.31	111	0.90	12.21	0.110	GÖ 480	4.06	54.37	0.94	3.1	0.022	0.762
E4	402	0.402	37.26	14.15	65.14	42.94	45.34	0.66	0.77	140.32	108	0.86	11.88	0.110	GÖ 480	3.57	48.91	0.94	3.2	0.023	0.810
E5	445	0.445	41.24	12.79	67.28	46.34	41.23	0.55	0.68	155.33	105	0.82	11.55	0.110	GÖ 480	3.13	44.37	0.94	3.4	0.024	0.845
E6	488	0.488	45.23	11.66	69.11	49.85	37.78	0.47	0.60	170.34	102	0.78	11.22	0.110	GÖ 480	2.75	40.54	0.94	3.5	0.026	0.871
E7	531	0.531	49.21	10.71	70.67	53.44	34.85	0.40	0.53	185.35	99	0.75	10.89	0.110	GÖ 480	2.42	37.28	0.94	3.7	0.027	0.891
E8	574	0.574	53.20	9.91	72.02	57.10	32.34	0.35	0.48	200.36	96	0.72	10.56	0.110	GÖ 480	2.14	34.48	0.94	3.8	0.028	0.907
E9	617	0.617	57.18	9.22	73.20	60.80	30.15	0.30	0.43	215.37	93	0.70	10.23	0.110	GÖ 480	1.90	32.05	0.94	3.9	0.028	0.919
TIP	660	0.660	61.17	8.62	74.24	64.54	28.24	0.27	0.39	230.38	90	0.68	9.90	0.110	GÖ 480	1.69	29.94	0.94	4.1	0.029	0.930

The automatic geometry and computational grid generation was constructed by Tcl/Tk commands, written by scripts that are interpreted through the commercial program ICEM CFD®.

The Simulation performed for this study does not consider the tip clearance, this issue will be taken into consideration in future work [8]. Due to the fact that the flow field is repeated for each blade, it is not necessary to model the complete rotor for simulation. Therefore, the mesh is generated only in the field related to a blade, which represents 1/9 of the full domain (9 axial rotor blades).

In Figures 9a and 9b can be observed the periodic channel and complete rotor geometries.

The computational mesh was created in ICEM-CFD15.0®, it is unstructured with tetrahedral elements. Figure 10a it is presented the computational domain mesh refer to a blade.

The boundary conditions were interpreted by FLUENT-CFD 15® that solves the flow equations for the discretized domain. The inlet surface is define by the velocity inlet, barometric pressure is considered 0.0 Pa and turbulence intensity of 5%. In the outlet flow is considered the condition *outflow*. This condition allows rotation change the dynamic pressure on the rotor output n= 1770 rpm.

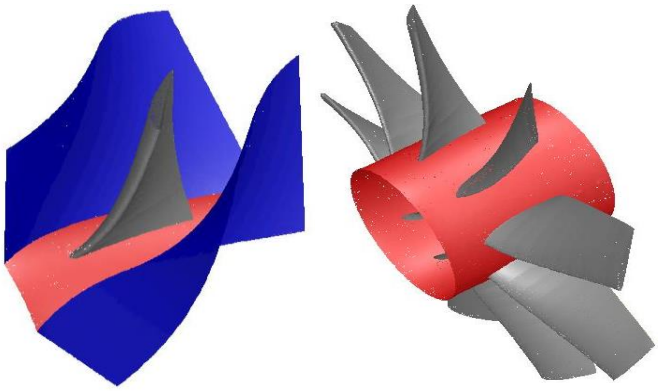

Fig. 9 Rotor of the axial fan without tip clearance; (a) periodic channel, (b) complete rotor.

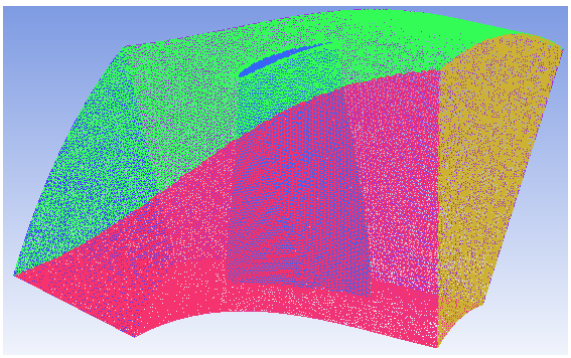

Fig. 10 Computational mesh of domain considering the fan geometry without tip clearance (2.062.186 elements).

The Figure 10, show the mesh with around two millions element, with refining of the elements in the leading and trailing. In the region near the wall, the elements size was calculated using the Y plus criterion around 20.

The Figure 11 shows the fan efficiency as a function of variation in mass considering the complete rotor for two rotations values. The curve in blue represented the nominal rotation and red one variation the rotation resulting in n=1947rpm, this analyze allowed check the methodology by design in the nominal point resulting the maximum efficiency in 91.40%. In this first approach we were not considered the effects of leakage and loss caused by tip clearance and also the geometric elements in the input and output of the rotor, resulting in high efficiencies

The Figure 12a present the pressure total contour in the rotor, can observed that the stagnation point is concentrated on leading edge, this fact mean that the stagger and attack angle were correctly calculated. The Figure 12b, show the streamlines in the blade, and can be observed few regions by separation boundary layer.

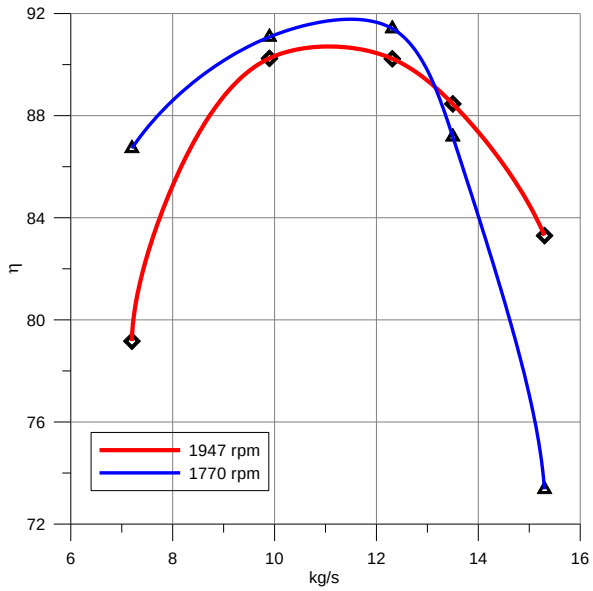

Fig. 11 Efficiencies variation vs. mass flow

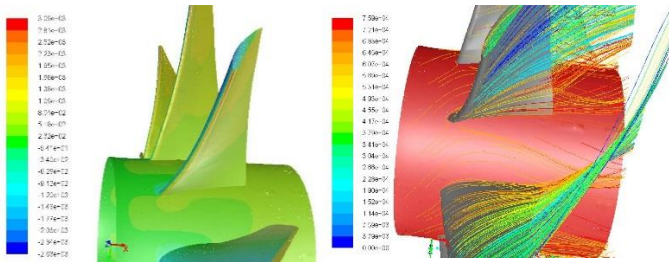

Fig. 12 (a) Pressure total contour in the rotor; (b) streamlines in the rotor.

The Tables V and VI show the result for hydraulic power, total pressure in function of the volumetric flow variations.

Table V Result values for n=1947 rpm

n=1947 rpm ρ=1.2 kg/m3					
ṁ [kg/s]	7.2	9.9	12.31	13.5	15.3
P_{Tin} [Pa]	569.13	685.98	984.78	1159.79	1436.86
P_{Tou} [Pa]	1643.72	1597.38	1691.82	1743.66	1832.34
η [%]	79.167	90.244	90.228	88.459	83.300
Q [m^3/s]	6.00	8.25	10.26	11.25	12.75
Δ_{PT} [Pa]	1074.59	911.40	707.04	583.87	395.48
Ph	6447.53	7519.05	7254.23	6568.54	5042.37

Table VI Result values for n=1770 rpm

n =1770 rpm, ρ=1.2 kg/m3					
ṁ [kg/s]	7.2	9.9	12.31	13.5	15.3
P_{Tin} [Pa]	427.81	661.21	957.63	1131.89	1403.91
P_{Tou} [Pa]	1283.11	1353.20	1453.61	1507.10	1600.25
η [%]	86.716	91.079	91.408	87.169	73.360
Q [m3/s]	6.00	8.25	10.26	11.25	12.75
Δ_{PT} [Pa]	855.295	691.990	495.974	375.213	196.336
Ph	5131.77	5708.92	5088.69	4221.14	2503.28

CONCLUSIONS

Based in the theory of lift and the free vortex was developed one design methodology for axial rotors. For geometry was created one script edited in TCL/Tk command for interpretation by software ICEM. For the calculation flow was used the fluent® CFD code. Efficiency results were obtained as a function of mass flow considering two rotations, and the 1770 nominal rotation. Results of local variables of pressure observe that the design methodology predicts minimal separation of regions of the boundary layers.

ACKNOWLEDGMENT

The authors acknowledge the BRENTECH ENERGIA S/A, and NEPEN – Center for Studies and Research Northeast, by Financial Support, Federal University of Pará - UFPA and Federal University Of Itajubá – UNIFEI by infrastructure to development of project.

REFERENCES

[1] R. Bran and Z. Souza. “Máquinas de Fluxo – turbinas, bombas e ventiladores”, Ao Livro Técnico S.A., Rio de Janeiro. 1969.
[2] C. Pfleiderer. “Die Kreiselpumpen für Flüssigkeiten und Gase” Springer – Verlag. 1961.
[3] J. D. Anderson Jr. “Fundamentals of Aerodynamics”, 2nd edition, McGraw-Hill International Editions, Aerospace Science Series. 1991.
[4] I. H. Abbott and A. E. Von Doenhoff. “Theory of Wing Sections”, Dover, New York. 1959.
[5] N. N. Kovalev. Hydroturbines, Design and Construction (Translated from Russia), Israel,Programme for Scientific Translations Jerusalém, 1965.
[6] Z. Souza. Dimensionamento de Máquinas de Fluxo – Turbinas, Bombas e Ventiladores,Editora Edgard Blücher Ltda, 1991.
[7] A. Sahili, B. Zogheib and R. Barron, "3-D Modeling of Axial Fans," Applied Mathematics, Vol. 4 No. 4, 2013, pp. 632-651. doi: 10.4236/am.2013.44088.
[8] H. Kumawat. “Modeling and Simulation of Axial Fan Using CFD”, Mechatronic and Manufacturing Engineering, vol. 8, no. 11, 2014, pp. 1858-1862.